A Role for the HOXB7 Homeodomain Protein in DNA Repair

Ethel Rubin,[1] Xinyan Wu,[1] Tao Zhu,[1] Joyce C.Y. Cheung,[2] Hexin Chen,[1] Annaka Lorincz,[1] Raj K. Pandita,[3] Girdhar G. Sharma,[3] Hyo Chol Ha,[4] Judith Gasson,[5] Les A. Hanakahi,[2] Tej K. Pandita,[3] and Saraswati Sukumar[1]

[1]Department of Oncology, Johns Hopkins University School of Medicine; [2]Department of Biochemistry, Bloomberg School of Public Health, Johns Hopkins University, Baltimore, Maryland; [3]Department of Radiation Oncology, Washington University School of Medicine, St. Louis, Missouri; [4]Department of Biochemistry, Georgetown University School of Medicine, Washington, District of Columbia; and [5]Department of Biological Chemistry, University of California, Los Angeles, California

Abstract

Homeobox genes encode transcription factors which function in body axis patterning in the developing embryo. Recent evidence suggests that the maintenance of specific HOX expression patterns is necessary for regulating the homeostasis of adult tissues as well. In this study, HOXB7 transformed human mammary epithelial cells, MCF10A, to grow in minimally supplemented medium, to form colonies in Matrigel, and display resistance to ionizing radiation. Searching for protein partners of HOXB7 that might contribute to resistance to ionizing radiation, we identified four HOXB7-binding proteins by GST pull-down/affinity chromatography and confirmed their interactions by coimmunoprecipitation *in vivo*. Interestingly, all four HOXB7-binding proteins shared functions as genomic caretakers and included members of the DNA-dependent protein kinase holoenzyme (Ku70, Ku80, DNA-PK$_{cs}$) responsible for DNA double-strand break repair by nonhomologous end joining pathway and poly(ADP) ribose polymerase. Exogenous and endogenous expression of HOXB7 enhanced nonhomologous end joining and DNA repair functions *in vitro* and *in vivo*, which were reversed by silencing HOXB7. This is the first mechanistic study providing definitive evidence for the involvement of any HOX protein in DNA double-strand break repair. [Cancer Res 2007;67(4):1527–35]

Introduction

HOX genes encode transcription factors that are characterized by a highly conserved trihelical homeodomain that binds to specific DNA sequences. A total of 39 *HOX* genes have been identified that are organized into four paralogous clusters, HOX-A to HOX-D, on autosomal chromosomes (1). The functions of homeodomain-containing proteins are diverse and include roles as both classical regulators of transcription and novel roles outside of transcriptional regulation. *HOX* genes are functionally important in anteroposterior patterning during embryogenesis, homeostasis in adult tissue, cell to cell interactions, and cell to extracellular matrix interactions (reviewed in ref. 2). Examples of novel roles for homeodomain-containing proteins include the role of human proline-rich homeodomain protein, PRH (known as Hex in studies on hematopoiesis), which interacts with eIF4E to inhibit its mRNA nuclear-cytoplasmic transport function (3). Given that HOX proteins can bind to very similar sequences *in vitro* but exert diverse functions *in vivo*, a fundamental question is how each HOX protein achieves functional specificity. One hypothesis is that functional specificity is attained by physical interaction with various cofactors.

DNA double-strand breaks (DSB), caused by exposure to ionizing radiation (IR), certain chemicals, or occurring during replication, V(D)J recombination, and meiosis, pose a major challenge to the maintenance of genomic integrity. If they are left unrepaired, cell cycle arrest, apoptosis, or mitotic cell death ensues, whereas faulty repair can lead to neoplastic transformation (4, 5). Nonhomologous end joining (NHEJ) is the major mechanism for the repair of IR-induced DSB, and involves the DNA end-binding heterodimer, Ku70/Ku80, the DNA-dependent protein kinase (DNA-PK), the *XRCC* gene product, and DNA ligase IV (6). The Ku antigen binds to and recruits DNA-PK to sites of DNA strand breaks, where DNA-PK is activated to participate in DNA repair. HOXC4 and HOXD4, along with homeodomain-containing proteins Octamer transcription factors 1 and 2, and Dlx2, interact with the COOH terminus of the Ku antigen causing their recruitment to broken DNA ends and phosphorylation by DNA-PK (7). However, the functional significance of this interaction is not known.

Another protein that contributes to genomic stability is poly(ADP) ribose polymerase (PARP). PARP catalyzes the transfer of polymers of ADP-ribose from NAD+ onto protein targets (8, 9), and regulates both cell survival and cell death programs. A recent study has shed some light on their involvement in DSB repair mediated by NHEJ and by homologous recombination (HR). Hochegger et al. (8) showed that PARP-1(−/−) mutant chicken cells have reduced levels of HR and are sensitive to various DSB-inducing genotoxic agents. Interestingly, this phenotype is strictly dependent on the presence of Ku70. PARP-1/KU70 double mutants are proficient in the execution of HR and display an elevated resistance to DSB-inducing drugs. These results suggest that PARP might function by minimizing the suppressive effects of Ku and the NHEJ pathway on HR.

In this study, we found that HOXB7 has the ability to confer both a transformed phenotype and resistance to IR in cultures of human mammary epithelial cells (HMEC), MCF10A. A search for protein interaction partners for HOXB7 that might contribute to this transformation led to the identification of the DNA repair proteins, Ku70, Ku80, the catalytic subunit of DNA-PK (DNA-PK$_{cs}$), and PARP. This, among other functions, suggests a role for HOXB7 in DNA repair through NHEJ. We present evidence to indicate that interaction between HOXB7 and the Ku antigens is functionally significant because HOXB7 expression enhances NHEJ, DNA-PK activity, and DNA damage repair in mammalian cells.

Note: Supplementary data for this article are available at Cancer Research Online (http://cancerres.aacrjournals.org/).

E. Rubin and X. Wu contributed equally to this work.

Requests for reprints: Saraswati Sukumar, Sidney Kimmel Comprehensive Cancer Center, 1650 Orleans Street, Room 410, Baltimore, MD 21231-1000. Phone: 410-614-2479; Fax: 410-614-4073; E-mail: saras@jhmi.edu.

doi:10.1158/0008-5472.CAN-06-4283

Materials and Methods

Cell culture, plasmids, transfections, and antibodies. Breast cancer cell lines were obtained from the American Type Culture Collection (Manassas, VA) and cultured as follows: SKBR3 cells in McCoy's 5A medium containing 15% fetal bovine serum (FBS), MDA-MB-231, MDA-MB-468, and MCF-7 cells in DMEM supplemented with 10% FBS. HMECs, MCF10A, and MCF12A, were cultured as described (10). Chinese hamster ovary (CHO) cells were cultured in DMEM/F-12 medium containing 10% FBS. All plasmids were sequenced to verify fidelity. FLAG-tagged or green fluorescent protein (GFP)–tagged HOXB7 or vector-transfected cells were selected in 800 μg/mL of G418-containing medium and cell clones were analyzed for expression of the fusion protein by Western blot and fluorescence microscopy. Expression vectors for Fl-tagged HOXB7 and mutants have been previously described (11). Transfections were done using Genejammer (Stratagene, La Jolla, CA). Transfection in MCF10A cells was done using Effectene (Qiagen, Valencia, CA) according to the manufacturer's instructions. His-tagged Ku70 and Ku80 expression plasmids were provided by Dr. Kathrin Muegge (National Cancer Institute, Bethesda, MD) and PARP-pCR3.1 was provided by Dr. Solomon Snyder (Johns Hopkins University School of Medicine, Baltimore, MD). SDS-PAGE and Western blots were done as described (12). The following monoclonal antibodies were used for protein detection by immunoblot: anti-FLAG M2 (Sigma, St. Louis, MO), PARP (clone C-2-10; Invitrogen, Carlsbad, CA), DNA-PK_{cs} (clone G-4; Santa Cruz Biotechnology, Santa Cruz, CA), Ku70 (clone 2C3.11; Novus Biologicals, Littleton, CO), Ku86 (clone B-1; Santa Cruz Biotechnology), Living Colors A.v. (clone JL-8; Clontech, Mountain View, CA) for detection of YFP and HOXB7-YFP, and GST goat polyclonal antibody (GE Healthcare, Piscataway, NJ).

Cell proliferation assays. MCF10A cells stably expressing HOXB7-Fl or vector control cells were grown in RPMI supplemented with 1% or 10% FBS, adherent cells were fixed in 10% formalin for 20 min, stained with 0.1% crystal violet, and lysed in 10% acetic acid. Colorimetric measurements were done using a microplate reader (Molecular Devices, Sunnyvale, CA) at 590 nm. Measurements were done in triplicate and the experiment was repeated thrice. Growth in and on Matrigel was assessed as described in ref. 13. Colony formation in Matrigel was assessed after 1 week. The number of colonies containing >200 cells was counted. Cells grown on Matrigel were assessed for the formation of three-dimensional structures 3 weeks after seeding. The morphology of the structures formed using MCF10A-vec and those formed by MCF10A-Fl-HOXB7 cells were compared and photographed under phase contrast at 20× magnification.

GST-HOXB7 affinity chromatography and identification of GST-HOXB7–binding proteins. GST-HOXB7 was expressed as previously described (11). The GST and GST-PRL3 expression plasmids were provided by Dr. Bert Vogelstein (Johns Hopkins University School of Medicine). Quantitation of GST or GST fusion proteins was done by silver staining SDS-PAGE gels using bovine serum albumin as a standard. Soluble fusion proteins, used as controls on protein gels, were eluted from the Sepharose beads with 25 mmol/L of glutathione (Sigma)/PBS (pH 8.0). Cell protein extracts were prepared from SKBR3, MCF10A, MCF-12A, MDA-MB-231 by scraping cells in 500 μL of EBC lysis buffer [50 mmol/L Tris-HCl (pH 8.0), 120 mmol/L NaCl, 0.5% NP40] supplemented with complete protease inhibitor cocktail (Roche, Indianapolis, IN). All cell extracts were precleared by prior incubation for 1 h with 5 μg of GST-Sepharose. For affinity chromatography, 5 μg (50–100 μL) of GST-HOXB7-Sepharose or control fusion protein was mixed for 2.5 h at 4°C with 5 mg of cell protein extracts. The beads were washed five times with 1 mL of EBC cell lysis buffer and eluted in 25 mmol/L glutathione/PBS (pH 8.0). Eluates were divided into two aliquots for protein staining or Western blot following SDS-PAGE. Protein identities were determined by one of two methods: direct sequencing from Coomassie blue–stained polyvinylidene difluoride (PVDF) membranes or peptide mass fingerprinting from tryptic peptides of Coomassie blue–stained bands on the gel, both done at the Stanford PAN facility (Palo Alto, CA). All protein identifications were confirmed by immunoblotting with corresponding antibodies.

Coimmunoprecipitation. For coimmunoprecipitation of HOXB7-binding proteins from SKBR3 cells expressing HOXB7-YFP or Fl-tagged HOXB7, 1 to 2 mg of cell protein extracts prepared as described above, were precleared (12) and subjected to immunoprecipitation for 2.5 h at 4°C with the following antibodies: full-length A.v. polyclonal antibodies (Clontech) for immunoprecipitation of HOXB7-YFP, or anti-FLAG polyclonal antibodies (Sigma) for precipitation of FL-HOXB7 complexes according to the suggestions of the manufacturer. Complementary coimmunoprecipitation of HOXB7-YFP with its binding proteins was done with monoclonal antibodies to human DNA-PK_{cs} and human Ku86 (clones H-163 and C-20, respectively; Santa Cruz Biotechnology) as described (12). To verify the interaction between endogenous HOXB7 with Ku70, Ku80, and DNA-PK under physiologic conditions and the effect of DNA depletion, 1 to 2 mg of whole cell lysates of MCF-7 (with or without ethidium bromide) were subjected to immunoprecipitation with Ku70 and Ku80 antibodies, the immune complexes were loaded onto 4% to 12% NuPAGE gels (Invitrogen) and immunoblotted with anti-HsKu70 (clone 2C3.11; Novus Biologicals), Ku86 (C-20; Santa Cruz Biotechnology), or anti-HOXB7 rabbit polyclonal antibodies (Invitrogen).

DNA repair and cell survival assays. Plasmid end-joining assays were done essentially as described in ref. 14. Briefly, nuclear extracts of SKBR3-HOXB7-YFP or vector-transfected cells were prepared with NE-PER Reagent (Pierce, Rockford, IL). Four micrograms of nuclear extracts were mixed with 0.25 μg of *Eco*RV- or *Bam*HI-cut pCDNA3, and digested for 1 h at 25°C in a buffer containing 20 mmol/L of Hepes-KOH (pH 7.5), 10 mmol/L of $MgCl_2$, and 80 mmol/L of KCl. The reaction was stopped with the addition of 2 μL of 5% SDS, 2 μL of 0.5 mol/L EDTA, and 1 μL of 10 mg/mL proteinase K and incubation at 37°C. Half of each reaction was resolved by electrophoresis on agarose gels. UV detection and densitometric quantitation was done using EagleEye Software. All experiments were done in duplicate and repeated twice. Relative NHEJ activity was obtained by calculating mean densitometric units of all the end-joined products on the gel.

Cell survival following gamma irradiation, measurements of mitotic indexes and determination of G_1 and G_2-type chromosomal aberrations after DNA damage. These experiments were done as described in ref. 15. Cells in plateau phase were irradiated with 3 Gy, subcultured, and examined for G_1-type aberrations at metaphase. All categories of asymmetric chromosome aberrations were scored: dicentrics, centric rings, interstitial deletions/acentric rings, and terminal deletions. For G_2-type aberrations, cells in exponential phase growth were irradiated with 1 Gy gamma irradiation. Metaphases were harvested 45 and 90 min following irradiation and examined for chromatid breaks and gaps. Fifty metaphases were scored for each postirradiation time point.

DNA-PK assay. Cell extracts were prepared as follows: MDA-MB-435 cells, cultured as monolayers, were harvested using a cell scraper, washed twice in PBS, snap-frozen on dry ice and stored at −80°C. Frozen cell pellets were resuspended in 70 to 90 μL of hypotonic lysis buffer [10 mmol/L Tris (pH 8.0), 1 mmol/L EDTA], incubated on ice for 20 min, and then subjected to vigorous vortexing for 30 s. High salt buffer [83.5 mmol/L Tris (pH 8.0), 1.65 mol/L KCl, 3.3 mmol/L EDTA, 1 mmol/L DTT] was added to 20% of total volume followed by incubation on ice for 20 min. Cell debris was removed by centrifugation (16,500 × *g*, 10 min, 4°C) and the resulting supernatant was collected as an extract. KCl was added to a final concentration of 0.5 mol/L, 25 μL of DEAE Sepharose resin (GE Healthcare) was added to remove DNA and the sample was rotated for 30 min at 4°C. DEAE Sepharose was removed by centrifugation and the sample was dialyzed against 20 mmol/L of Tris (pH 8.0), 0.1 mol/L of KHAc, 10% glycerol, 0.5 mmol/L of EDTA, and 1 mmol/L of DTT. DNA-PK assays were done in duplicate according to the instructions of the manufacturer (Promega, Madison, WI) using 40 μg of the extract/assay. Three separate assays were done. The results were calculated as mean ± SD. Two-tailed Student's *t* test was done to calculate *P* values.

Small interfering RNA expression construct and transfection. The small interfering RNA (siRNA) sequences used for targeting human *HOXB7* were 5′-ATATCCAGCCTCAAGTTCG-3′ and 5′-ACTTCTTGTGCGTTTGCTT-3′. Oligonucleotides encoding siRNAs (Invitrogen) were annealed and ligated into pSilencer-U6 vector (Genscript, Piscataway, NJ). The two HOXB7

siRNA expression plasmids were mixed 1:1 for transfection. Plasmids (1 μg/well) containing HOXB7 siRNA or siRNA of the scrambled sequence (control) was transfected into six-well plates by use of Effectene (Qiagen) for 24 h.

Measurement of DNA DSBs. Assay of DNA DSB repair activity following DNA damage induced by IR was done under nondenaturing conditions by a standard procedure using pulsed-field gel electrophoresis (PFGE) as described previously (16, 17). Cells kept on ice received a gamma radiation dose of 50 Gy. Immediately following irradiation, the cells were placed in medium at 37°C, incubated at 37°C for various time periods, trypsinized, washed, and embedded in agarose plugs, lysed, and digested with proteinase K. Plugs were washed in TE buffer [10 mmol/L Tris-HCl, 1 mmol/L Na_2 EDTA (pH 8)] and PFGE was carried out with a contour-clamped homogeneous electric field in 0.8% agarose gels. The gels were run at 14°C with linearly increasing pulse times as described (16, 17). Gels were stained with ethidium bromide and photographed with a charge-coupled device camera system under UV transillumination. Quantitative analysis to determine the fraction of DNA entering the gel provided a measure for the relative number of DSBs. The control cell DNA was normalized to zero and 100% was assigned to DNA of cells treated with 50 Gy with no repair.

Results

HOXB7 elicits a transformed phenotype in MCF10A cells. Overexpression of HOXB7 enabled nontumorigenic breast cancer cells, SKBR3, to form well-vascularized tumors in immunodeficient mice (18). To investigate whether HOXB7 expression transforms normal breast epithelial cells, a FLAG-tagged (Fl) HOXB7 expression plasmid was transfected into immortalized HMECs, MCF-10A, and pooled G418-selected colonies stably expressing HOXB7 were tested for alterations in growth properties compared with the vector-transfected cells (Fig. 1*A* and *B*). MCF10A cells require a highly growth factor–supplemented medium for optimal growth (19). In low growth nutrient RPMI with 10% or 1% serum supplementation, unlike vector-control cells, MCF10A-Fl-HOXB7 cells displayed a continued ability to proliferate (Fig. 1*A*). Grown in Matrigel in complete medium, in contrast to the minute colonies formed by MCF-10A-vec–transfected cells (Fig. 1*C, 1*), MCF10A-Fl-HOXB7 cells formed 200 to 300 cells, anchorage-independent colonies (Fig. 1*C, 2*) within 3 weeks. Grown on Matrigel-coated plates, MCF10A cells formed discrete acini-like structures with a hollow lumen (Fig. 1*C, 3*), whereas MCF10A-Fl-HOXB7 cells displayed large irregular solid colonies with cells pushing haphazardly into the surrounding extracellular matrix (Fig. 1*C, 4*). Taken together, the results indicate that the MCF10A-Fl-HOXB7 cells exhibit a transformed phenotype like that of MCF10A cells expressing RAS or HER2/neu oncogenes (13, 19).

HOXB7 increases resistance to IR. Some activated oncogenes render cells resistant to radiation whereas others enhance their susceptibility to IR. The molecular basis of sensitivity to IR is a complex product of cellular responses; loss of cell cycle checkpoints may result in increased sensitivity, particularly if the checkpoint controls G_2 transitions. To determine the effects of overexpressed HOXB7 on the response to IR exposure, several tests were done. Clonogenic survival assays were done using stably transfected MCF10A cells (Fig. 1*B*). Upon exposure to low-dose gamma radiation, MCF10A-Fl-HOXB7 cells had an ~2-fold enhanced survival advantage over the vector-transfected and parental MCF10A cells (Fig. 2*A*). Similar results were obtained with SKBR3 cells (Fig. 2*B*) stably expressing HOXB7-YFP as shown by immunoblotting (Supplementary Fig. S1).

We also examined G_1-type (Fig. 2*C*) and G_2-type (Fig. 2*D*) chromosomal aberrations in metaphase spreads from subcultured

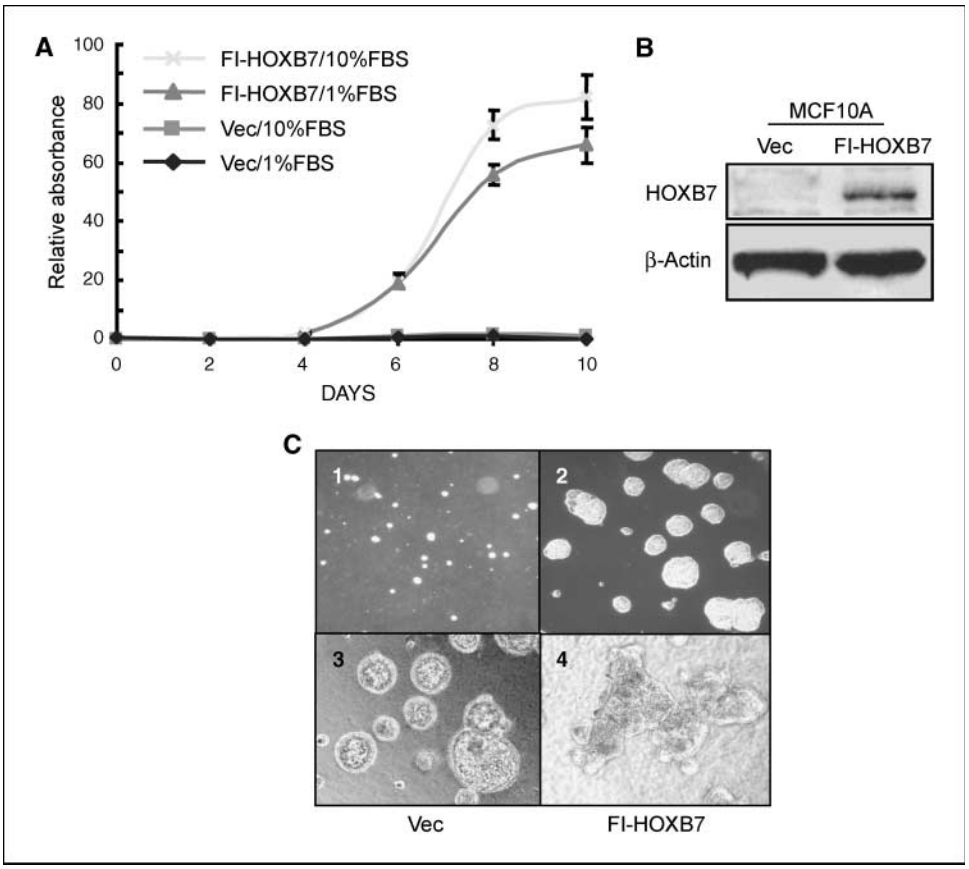

Figure 1. Overexpression of HOXB7 can confer a transformed phenotype on MCF10A. *A,* MCF10A cells stably expressing HOXB7 or vector control cells were grown in RPMI supplemented with 1% or 10% FBS, and the cells were stained with crystal violet. Colorimetric measurements were done in triplicate for samples and each experiment was repeated thrice. *B,* Western analysis using anti-HOXB7 antibodies confirmed its expression in the stably transfected MCF10A-Fl-HOXB7 cells. The same blot reprobed with anti–β-actin antibodies provided loading controls. *C, (1)* MCF10A-vec cells remaining as 2 to 10 cell clusters grown in Matrigel; *(2)* MCF10A-Fl-HOXB7 cells formed large, anchorage-independent colonies when grown in Matrigel; *(3)* MCF10-vec cells formed acinar structures with hollow lumen; and *(4)* MCF10A-Fl-HOXB7 grew as irregular, solid colonies when grown on the surface of Matrigel. Phase contrast (magnification, ×20).

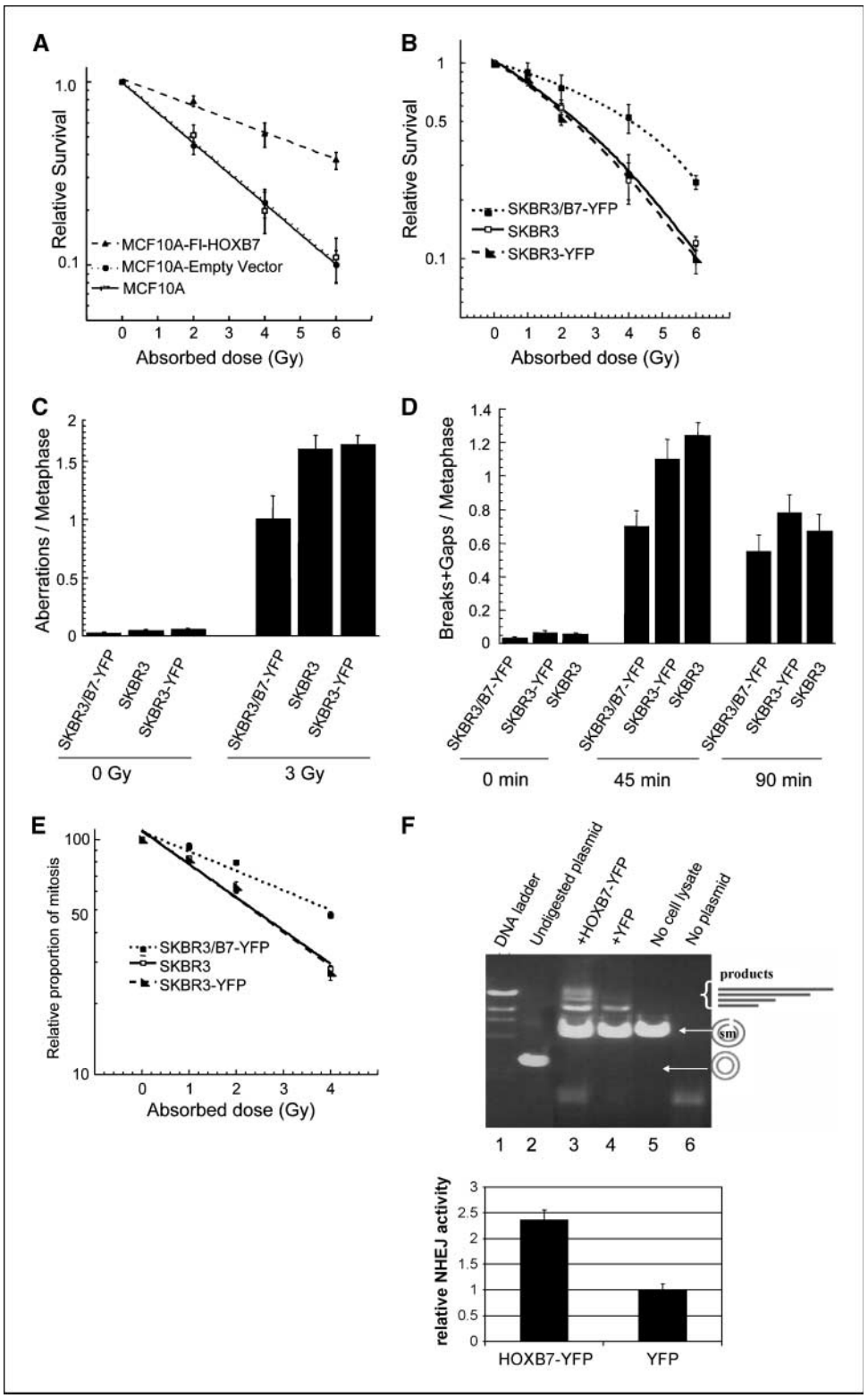

Figure 2. Altered response of HOXB7-expressing MCF10A and SKBR3 cells to IR. *A* and *B,* clonogenic survival assays. Percentage of survival of MCF10A parental cells and MCF10A-FI-HOXB7 or MCF10A-vec (*A*), or SKBR3 parental cells, SKBR3-HOXB7-YFP, SKBR3-YFP cells (*B*) irradiated at the indicated doses was calculated and compared with mock-irradiated (0 Gy) controls. *C,* G_1-type chromosomal aberrations after radiation treatment. The frequency of aberrations following irradiation with 3 Gy was calculated in parental SKBR3, SKBR3-HOXB7-YFP, and SKBR3-vec cells. *D,* G_2-type chromosomal aberrations after radiation treatment. Number of chromatid breaks and gaps in metaphases were scored for SKBR3-HOXB7-YFP cells and compared with those of SKBR3-YFP and parental SKBR3 controls. *E,* mitotic index after radiation treatment. Parental SKBR3, SKBR3-YFP, and SKBR3-HOXB7-YFP cells in exponential phase were irradiated with increasing doses of gamma radiation and then examined for the frequency of mitotic cells. *Columns,* mean value from three independent experiments; *bars,* SD. For each experiment, 200 metaphases were scored. *F,* HOXB7 stimulates DNA repair *in vitro* and *in vivo*. Plasmid end-joining assays were done. Nuclear extracts of SKBR3 cells expressing HOXB7-YFP or YFP alone were mixed with 0.25 μg of blunt-digested pCDNA3.0 in a plasmid end-joining reaction. Products were resolved on 0.7% ethidium bromide–stained agarose gels. *Lane 1,* DNA ladder; *lane 2,* undigested pCDNA3.0; *lane 3,* digested plasmid plus SKBR3-HOXB7-YFP nuclear extract; *lane 4,* digested plasmid plus SKBR3-YFP nuclear extract; *lane 5,* digested plasmid plus extraction buffer; *lane 6,* SKBR3-HOXB7-YFP nuclear extract minus plasmid. Band intensities were quantitated on Eagle Eye software. *Columns,* mean from two separate analyses; *bars,* SD.

SKBR3 cells at various time points postirradiation (15). Cells in plateau phase were irradiated with 3 Gy, subcultured and examined for G_1-type aberrations at metaphase. The frequency of aberrations was calculated in parental SKBR3, SKBR3-HOXB7-YFP, and SKBR3-vec cells and was significantly lower in SKBR3-HOXB7-YFP cells than in the other two groups (Student's *t* test, $P < 0.05$). For G_2-type aberrations, cells in exponential phase growth were irradiated with 1 Gy gamma radiation. Metaphases were examined for chromatid breaks and gaps. Fifty metaphases were scored for each post-irradiation time point. Results for SKBR3-HOXB7-YFP–expressing cells were compared with those of vector-transfected (SKBR3-YFP) and parental (SKBR3) controls. SKBR3-HOXB7-YFP cells showed a

significant decrease in G_2-type chromosome aberrations as compared with parental control cells (Student's t test, $P < 0.035$). These cells possessed an intact G_2-M checkpoint (data not shown), although their elevated mitotic index (Fig. 2*E*) seems to indicate enhanced recovery and repair of DNA damage. The nature of the protection against radiation conferred by HOXB7 in these assays suggests that HOXB7 may affect DNA repair kinetics through the NHEJ pathway.

To explore this further, we tested the DNA repair activities of HOXB7-containing nuclear extracts *in vitro* by plasmid end-joining assays (14). This analysis revealed that expression of HOXB7-YFP in SKBR3 cells stimulated the end-joining activity almost 2.5-fold (Fig. 2*F*). These results were verified by knockdown of endogenous HOXB7 expression in breast cancer cells, MDA-MB-468, using antisense constructs. Transient transfection of HOXB7 antisense plasmids into MDA-MB-468 cells could suppress the expression of HOXB7 (>75%), and reduce NHEJ activity by ~1.6-fold (data not shown). These results suggest a role for HOXB7 in stimulating DNA repair, and raise the possibility that it occurs through NHEJ.

HOXB7 interacts with DNA repair proteins. To investigate whether HOXB7 plays a role in NHEJ, we attempted to identify proteins interacting with HOXB7 in breast cells. Cell extracts of

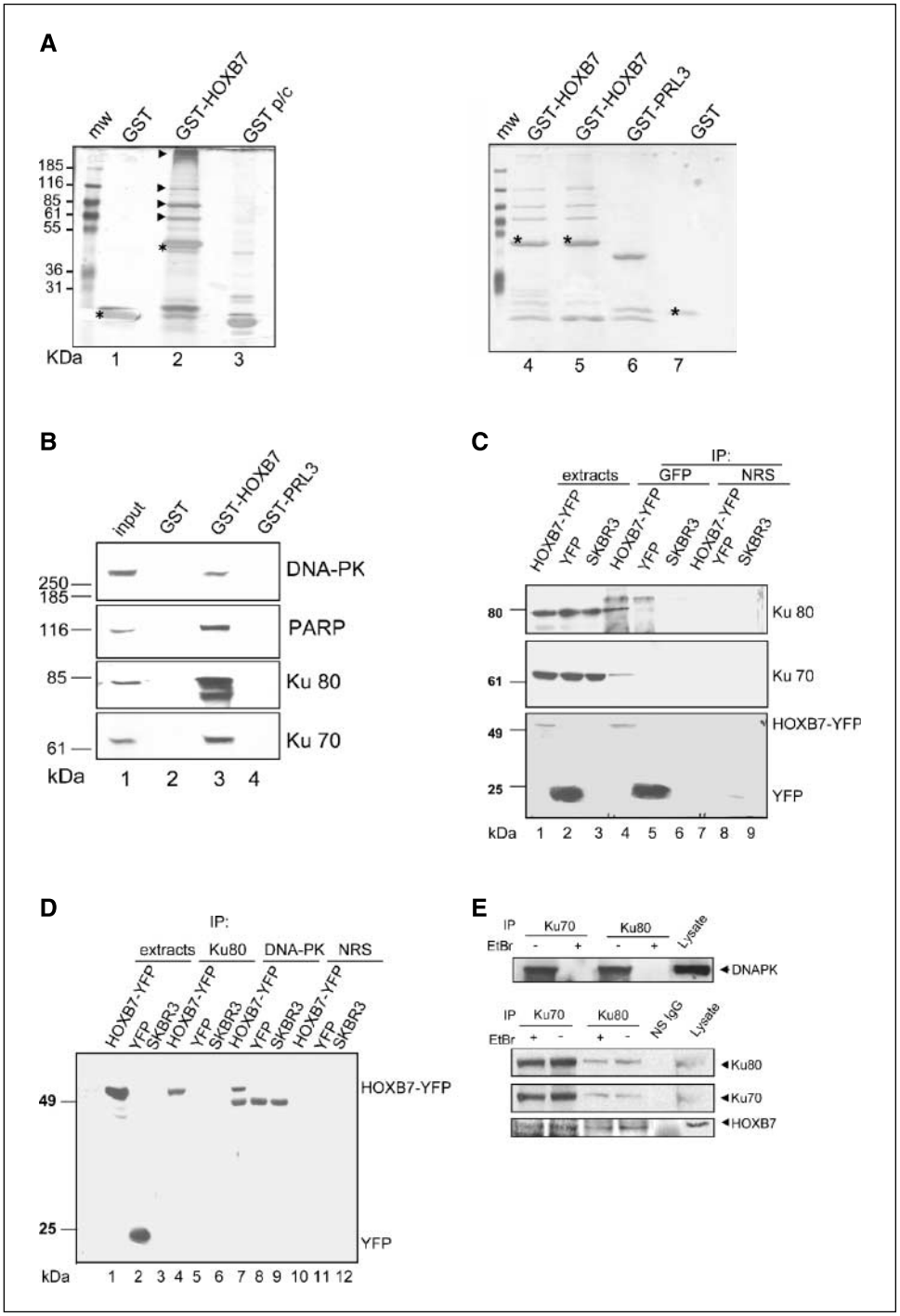

Figure 3. Identification and analysis of HOXB7 interacting proteins. *A,* affinity chromatography. GST-HOXB7 interacting proteins from SKBR3 cells (*lanes 1–3,* silver-stained gel; *lane 4,* Coomassie-stained PVDF membrane) or MCF10A cells (*lanes 5–7,* Coomassie-stained PVDF membrane). *Lanes 1* and *7,* proteins bound to GST alone (*GST*); *lane 3,* proteins bound to GST alone during the preclearing (*GST p/c*) step; *lane 6,* proteins bound to an unrelated control (*GST-PRL3*). *, positions of GST (*lane 1* and *7*) and GST-HOXB7 (*lanes 2, 4*, and *5*). *B,* immunoblot confirmation of HOXB7-interacting proteins. Proteins which bound to GST-HOXB7 (*lane 3*) or control matrices (*lanes 2* and *4*) were eluted, separated by SDS-PAGE, and transferred to nitrocellulose and immunoblotted with antibodies to the DNA-PK_{cs}, PARP, Ku86, and Ku70. SKBR3 cell extracts (100 μg of total extract, 2% of input; *lane 1*) served as a positive control for proteins detected by immunoblot. *C,* coimmunoprecipitation of PARP, Ku80, and Ku70 with HOXB7-YFP in SKBR3 cells. SKBR3 cells were stably transfected with HOXB7-YFP (*lanes 1, 4*, and *7*) or YFP alone as a vector control (*lanes 2, 5*, and *8*) prior to immunoprecipitation with GFP antibodies and subsequent Western blot of precipitated proteins. Parental SKBR3 cells, which lack detectable HOXB7, were used as controls as well (*lanes 3, 6*, and *9*). *Lanes 1* to *3,* protein levels in 100 μg of total cell extracts (5% of input); *lanes 4* to *6,* proteins that precipitated with HOXB7-YFP or controls that did not express HOXB7 (SKBR3-YFP and parental cells). Normal rabbit serum (*NRS*) was used to control for specificity (*lanes 7–9*). *D,* coimmunoprecipitation of HOXB7-YFP with DNA-PK_{cs} and Ku80 in SKBR3 cells. Complementary immunoprecipitations to those in Fig. 3*C* were done using SKBR3 cells transiently transfected with HOXB7-YFP (*lanes 1, 4*, and *7*), YFP alone (*lane 2, 5*, and *8*), or SKBR3 parental cells, which do not express HOXB7 (*lanes 3, 6*, and *9*). Normal rabbit serum (*NRS*; *lanes 10–12*) was used as a nonspecific IgG control. *E,* DNA is not required for the interaction between HOXB7 and the DNA-PK complex. Extracts of MCF-7 cells were treated with ethidium bromide prior to coimmunoprecipitation with antibodies to Ku70 and Ku80, or p53 as a nonspecific IgG (*NS IgG*). Subsequent immunoblotting was done with the antibodies indicated (*right*). *Top,* effective blocking of the interaction between Ku70/80 and DNA-PK by using ethidium bromide depletion of DNA (positive control). *Bottom,* no effect of DNA depletion on the interactions between HOXB7 and Ku70 and Ku80.

SKBR3 (Fig. 3*A, lanes 2* and *4*) and MCF10A (Fig. 3*A, lane 5*) were fractionated by affinity chromatography on GST-HOXB7-Sepharose. Analysis of the proteins in column eluates by silver and Coomassie staining after SDS-PAGE revealed the presence of four polypeptides of approximate sizes of 70, 85, 110, and >250 kDa, which did not bind to the GST (*lanes 1* and *7*), or to the unrelated GST-fusion protein, GST-PRL3 (*lane 6*). Similar results were obtained with extracts of HMECs (MCF-12A) and breast cancer cells (MDA-MB-231; data not shown).

To identify the eluted proteins, several methods were used. Direct sequencing from PVDF membranes yielded results for the 85 kDa band, which identified Ku80 from an NH_2-terminal 17–amino acid sequence (VRSGNKAAVVLCMDVGF). For the 110 and 70 kDa protein bands, peptide mass fingerprints were obtained by MALDI-TOF and compared against those in public databases. Both ProFound and MS-FIT public database searches for the peptide mass maps obtained from the 110 and 70 kDa protein bands identified PARP and Ku70, respectively. Protein identities were confirmed by immunoblotting with antibodies against PARP, Ku80, and Ku70 (Fig. 3*B*). Because Ku70/80 are known binding subunits of DNA-PK, the high molecular weight band appearing at the top margin of the gel (>250 kDa) was predicted and confirmed as the DNA-PK_{cs} by immunoblot analysis (Fig. 3*B*). The finding of several components of the DNA-PK complex suggested that DNA repair observed in the experiments described above are most likely mediated by NHEJ. We therefore focused our efforts on understanding the interaction of HOXB7 with components of the NHEJ complex.

Next, to test these interactions in intact cells, the associations between HOXB7 and Ku70, Ku80, and DNA-PK_{cs} were analyzed *in vivo* by coimmunoprecipitation. A HOXB7-YFP fusion construct was stably introduced into the HOXB7-null breast cancer cell line, SKBR3. Fluorescence microscopy confirmed that HOXB7-YFP localized solely to the nucleus (data not shown). Immunoprecipitation with GFP antibodies (which also recognize the YFP variant) showed that Ku70 and Ku80 associated with HOXB7 *in vivo* (Fig. 3*C, lane 4*). Complementary immunoprecipitation using Ku80 (Fig. 3*D, lanes 4–6*) or DNA-PK_{cs} (Fig. 3*D, lanes 7–9*) antibodies confirmed the presence of HOXB7-YFP in their complexes (*lanes 4* and *7*) following transient transfection of this construct into SKBR3 cells. Identical results were obtained when Fl-HOXB7 (Fl-HOXB7pcDNA3) was transiently expressed in SKBR3 cells (data not shown). Complex formation was not affected by DNA damage from UV or IR (data not shown). To rule out the fact that these interactions were just the consequence of overexpressed HOXB7 protein, coimmunoprecipitation analyses were done using protein extracts of breast cancer cells, MDA-MB-435, which express detectable levels of endogenous HOXB7. The results showed that the same interaction between HOXB7 and Ku70/Ku80 occurs under physiologic conditions (data not shown).

The common DNA-binding properties of these proteins raised the possibility that the interactions observed above were mediated through DNA rather than through direct protein-protein interactions. We tested this possibility using two methods. First, DNase I had no effect on the binding of HOXB7 to Ku70/80 in HOXB7-transfected SKBR3 cells (Supplementary Fig. S2). This finding was also verified more stringently using extracts of MCF-7 cells which express endogenous HOXB7. As previously shown (20), treatment with an intercalating agent (ethidium bromide) effectively blocked the interaction between Ku70/80 and DNA-PK because this reaction was completely dependent on the presence of DNA (Fig. 3*E, top*). In contrast, depletion of DNA in the extracts using ethidium bromide did not reduce the interactions between endogenous HOXB7 and Ku70 or Ku80 (Fig. 3*E, bottom*). We also found no evidence for the interaction of HOXB7 with two other DNA-binding proteins, i.e., BRCA-1 and E2F1 (data not shown). These results suggest that the interaction between HOXB7 and Ku70 and Ku80 are, in all likelihood, specific and not mediated by DNA.

Because complexes formed by interactions between Ku70, Ku80, and DNA-PK_{cs} were well-established, we investigated the nature of these complexes with HOXB7 and the order of their formation.

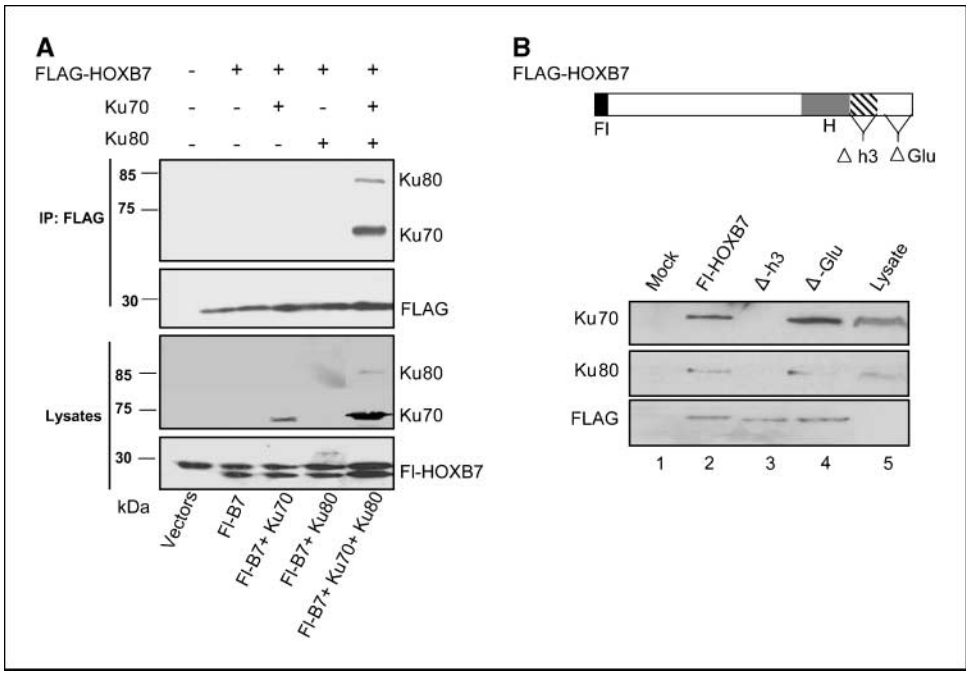

Figure 4. Analysis of HOXB7 complexes. *A,* Ku70/80 heterodimer formation is a prerequisite for HOXB7 binding. Fl-HOXB7 was transiently expressed in the CHO cells alone or with human Ku70 and/or human Ku80, coimmunoprecipitated with FLAG-antibodies, and immunoblotted with the antibodies indicated (*right*). Total protein lysates (100 μg; 5% of input). *B,* defining the region of HOXB7 that interacts with Ku70/80 proteins. *Top,* schematic representation of FLAG-tagged HOXB7 (*FLAG-HOXB7*), and deletion constructs. Locations of the FLAG tag (*Fl*), homeodomain (*H*), and deletions of the third helix (*Δh3*) of the homeodomain, and of the glutamic acid–rich tail (*ΔGlu*). *Bottom,* Fl-HOXB7, HOXB7-Δh3, and HOXB7-ΔGlu were transfected into SKBR3 cells, and cell lysates were subjected to coimmunoprecipitation with the anti-FLAG antibody, and then immunoblotted with the antibodies indicated (*left*).

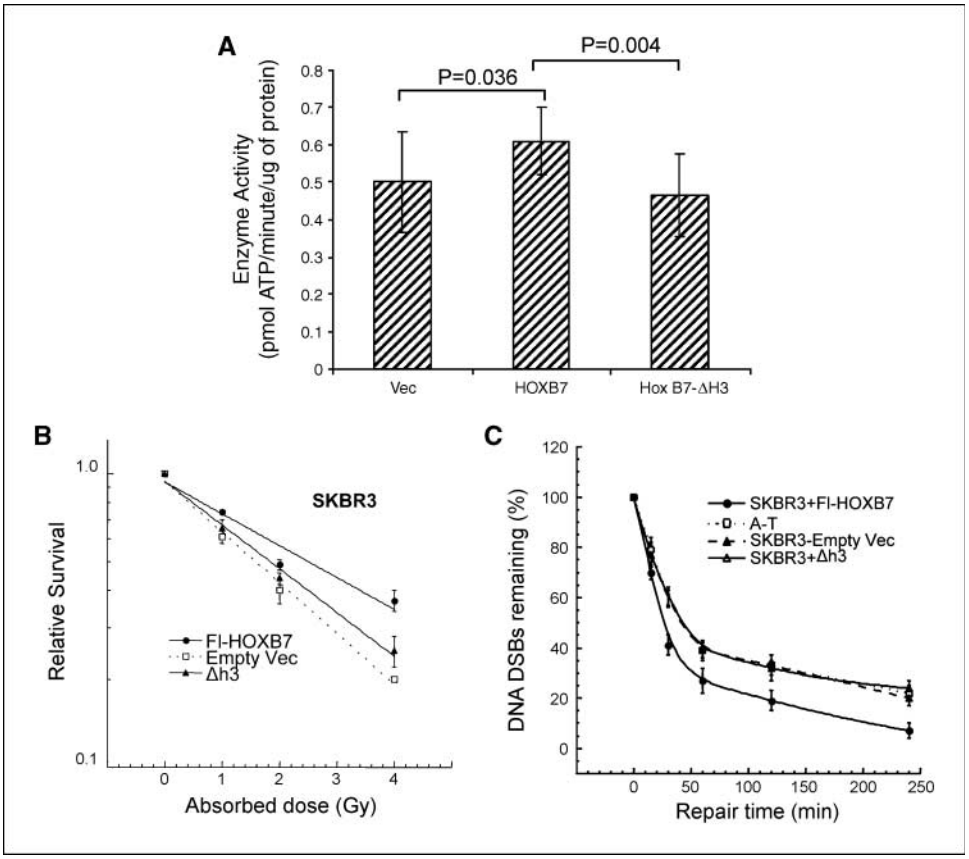

Figure 5. HOXB7 stimulates DNA-PK activity and the helix-3 domain is indispensable for HOXB7-mediated enhancement of cell survival and NHEJ. *A,* DNA-PK activity is enhanced in HOXB7-expressing cells. DNA-PK activity was measured in DNA-depleted whole cell extracts prepared from cells transiently transfected with either the empty vector or with plasmids expressing Fl-HOXB7 or HOXB7-Δh3. *Columns,* mean values of duplicate samples from three experiments; *bars,* SD. *B,* clonogenic survival assays. Survival of SKBR3 cells transiently transfected with Fl-HOXB7, HOXB7-Δh3, or the empty vector after irradiation were compared with mock-irradiated (0 Gy) controls. *C,* DNA DSB repair. Cells were irradiated with 50 Gy and lysed at different periods after irradiation. Control cells are repair-deficient ataxia telangiectasia cells (*AT*), GM5823. Unrepaired DNA breaks were measured under nondenaturing conditions. *Points,* means from three independent experiments; *bars,* SD.

Experiments introducing Fl-HOXB7 into CHO cells (Fig. 4*A*) showed that coexpression of human Ku70 and human Ku80 was required for the association of either Ku subunit with HOXB7. These results raise the possibility that Ku70/Ku80 heterodimer formation is a prerequisite for HOXB7 binding.

In order to define the region of HOXB7 that interacts with Ku70/80 proteins, full-length Fl-HOXB7 and HOXB7 with deletions of helix 3 of the homeodomain (HOXB7-Δh3) or of the glutamic acid tail (HOXB7-ΔGlu; Fig. 4*B, top*; ref. 11) were transfected into SKBR3 cells, and cell lysates were subjected to coimmunoprecipitation with FLAG antibody (Fig. 4*B, bottom*). The results showed that deletion of helix 3 from the homeodomain in HOXB7 (*lane 3*) completely abolished the interaction between HOXB7 and Ku70/80 proteins. In contrast, removal of the glutamic acid tail from HOXB7 (*lane 4*) did not affect the interaction. These results show that the integrity of the homeodomain is essential for the interaction between HOXB7 and Ku70/Ku80.

Expression of HOXB7 stimulates DNA-PK activity and enhances NHEJ. Because Ku70/80 is the DNA-binding subunit of DNA-PK, it is plausible that the observed interaction between Ku70/80 and HOXB7 may affect the catalytic activity of DNA-PK, and therefore NHEJ. To investigate the effect of HOXB7 expression on DNA-PK activity, MDA-MB-435 cells were transiently transfected with HOXB7 constructs (protein expression shown in Supplementary Fig. S3). As shown in Fig. 5*A*, the expression of HOXB7 resulted in an increase in DNA-PK activity ($P = 0.036$). Expression of HOXB7 lacking helix 3 of the homeodomain eliminated this effect, consistent with the finding that interaction between HOXB7 and Ku70/80 proteins is abolished by deletion of helix 3 from the homeodomain in HOXB7 (Fig. 4).

Because increased DNA-PK activity was abrogated by the deletion of helix 3 of HOXB7 (Fig. 5*A*), we further studied the effects of this deletion in clonogenic assays and in a DNA DSB repair assay. SKBR3 cells were transiently transfected with Fl-HOXB7, HOXB7-Δh3, or empty vector (Supplementary Fig. S4) and exposed to IR; survival of the cell clones was compared with mock-irradiated (0 Gy) cells. Unlike full-length HOXB7 protein, HOXB7-Δh3 was unable to efficiently protect cells from the effects of IR. The difference in cell survival postirradiation between cells with full-length and those with mutant HOXB7 was significant (Student's t test, $P < 0.05$; Fig. 5*B*). Thus, deletion of the h3 domain of HOXB7 eliminated protection against IR afforded by the full-length HOXB7 protein.

To determine if improved survival after radiation was a reflection of higher efficiency of repair of the DNA DSBs caused by the presence of HOXB7, SKBR3 cells transfected with Fl-HOXB7, HOXB7-Δ h3, or empty vector were used. An ataxia telangiectasia cell line, GM5823, was used as a known repair-deficient control. Cells were irradiated with 50 Gy and lysed at different intervals after irradiation. Unrepaired DNA breaks were resolved by PFGE under nondenaturing conditions. SKBR3 cells were as inefficient at DSB repair as the ataxia telangiectasia cells. Cells overexpressing HOXB7 had the least amount of residual DNA DSBs. The effect of wild-type HOXB7 on residual DNA damage in cells was significant (Student's t test, $P < 0.05$). Deletion of the h3 domain of HOXB7 abrogated the protective effect (Fig. 5*C*). Collectively, these experiments provide evidence that HOXB7 plays an important role in DNA DSB repair. Furthermore, the h3 domain of HOXB7 is essential for the enhancement of DNA DSB repair through NHEJ.

Knockdown of endogenous *HOXB7* reduces the efficiency of DNA repair. Our results provide strong support that HOXB7

associates with members of the DNA-PK holoenzyme. Initial findings had pointed to enhanced DNA repair capability in HOXB7-overexpressing cells (Figs. 2 and 5). To further test the relevance of these findings and the contribution of HOXB7 to DNA repair, survival after IR exposure following suppression of HOXB7 expression using siRNA was investigated. The expression of transfected *HOXB7*-specific siRNA into both MCF-7 (Supplementary Fig. S5) and MDA-MB-468 cells (Supplementary Fig. S6) reduced clonogenic survival significantly ($P < 0.01$; Fig. 6*A* and *B*). Next, chromosomal aberrations were analyzed at metaphase after irradiation of MDA-MB-435 cells with or without reduced levels of HOXB7 (Supplementary Fig. S7). All categories of asymmetric chromosome aberrations were scored. The frequency of chromosomal aberrations was higher in cells with reduced levels of HOXB7, indicating defective repair of chromosome damage (Fig. 6*C*). Cells with HOXB7 knockdown showed significant differences ($P < 0.01$) in chromosomal aberration frequencies compared with control cells (Fig. 6*C*). To further investigate the capacity of the G_1-arrested cells to repair DSBs induced by IR, and to determine if this effect was mediated by HOXB7, PFGE was done on DNA from gamma-irradiated MDA-MB-435 cells transfected with scrambled siRNA or with *HOXB7*-specific siRNA (Supplementary Fig. S7). Indeed, the specific siRNA treatment significantly ($P < 0.04$) increased the level of unrepaired DNA DSB (Fig. 6*D*). Collectively, these data strongly suggest that HOXB7 could protect cells against DNA damage induced by IR exposure, possibly by conferring a higher efficiency of DNA DSB repair.

Discussion

This study reports that HOXB7 is capable of transforming HMECs and of conferring resistance to IR. Resistance to IR seems to be through the binding of HOXB7 to proteins involved in DNA DSB repair, i.e., Ku70, Ku80, and DNA-PK_{cs}. This is the first report demonstrating that HOXB7 acts as an oncogene, interacts with members of the DNA-PK holoenzyme, and plays a role in DNA DSB repair.

It is intriguing that HOXB7 is not only a transcriptional regulator, but also functions in DNA DSB repair. We have shown that one possible mechanism is by direct or indirect enhancement of the activity of a key enzyme, DNA-PK. Our results do not, at the present time, rule out transcriptional regulation of DNA repair genes as a possible mechanism. There is precedence for this premise. For example, when the *Pem* homeodomain–containing gene was expressed in murine Sertoli cells, it increased the number of DNA single-strand and double-strand breaks in the neighboring cells by regulating the expression of genes which affect DNA repair or chromatin remodeling (21).

Recent studies suggest that several other homeodomain-containing proteins may also play roles outside of transcriptional regulation, or have homeodomain-independent functions. Thus, the human proline-rich homeodomain protein, PRH (known as Hex in hematopoietic studies), interacts with eIF4E and inhibits its mRNA nuclear-cytoplasmic transport function (3). In addition, a variant of the CSX1 (CSX1b) protein lacking the homeodomain, retained its function (22), and a splice variant of *Meis2* (Meis2e)

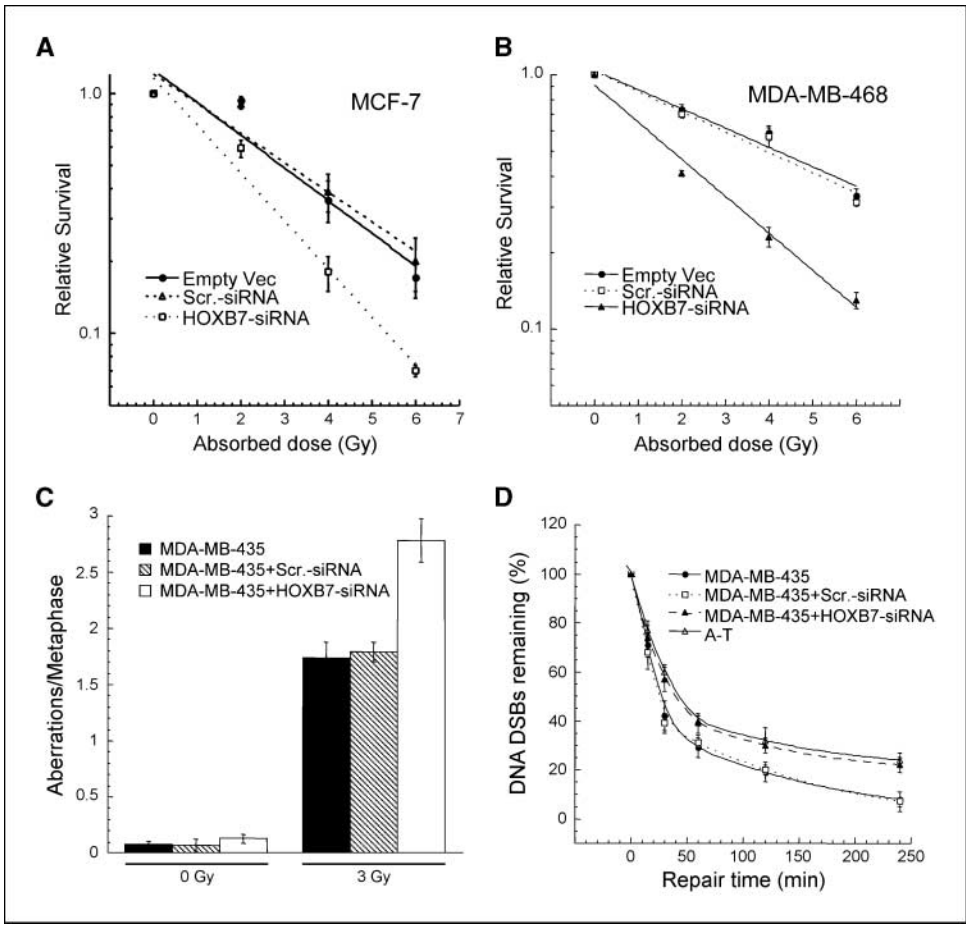

Figure 6. Knockdown of endogenous HOXB7 reduces DNA repair efficiency. *A* and *B,* clonogenicity after exposure to radiation of MCF-7 and MDA-MB-468 cells transfected with HOXB7-specific siRNA. Clonogenic survival assays of MCF-7 (*A*) or MDA-MB-468 (*B*) cells stably transfected with plasmids expressing either scrambled sequence siRNA (*Scr.-siRNA*) or HOXB7-specific siRNA (*HOXB7-siRNA*) were done. Survival was calculated on day 14 for MCF-7 and on day 10 for MDA-MB-468 relative to mock-irradiated (0 Gy) controls. *C,* analysis of chromosome damage and repair in MDA-MB-435 cells with or without reduced levels of HOXB7. Cells with HOXB7 knockdown (*HOXB7-siRNA*) showed significant differences in chromosomal aberration frequencies per metaphase compared with control cells (*Scr.-siRNA*). *D,* knockdown of HOXB7 reduces level of DNA DSB repair in MDA-MB-435. Cells with and without reduced levels of HOXB7 by transfection of HOXB7-specific (*HOXB7-siRNA*) or scrambled siRNA (*Scr.-siRNA*) along with parental cells were irradiated with 50 Gy and unrepaired DNA breaks were measured by PFGE. *Points,* means from three independent experiments; *bars,* SD.

lacking a complete homeodomain possessed some regulatory function (23). Studies in Drosophila have shown that the fushi tarazu protein has homeodomain-independent functions (24). Thus, novel functions of homeobox proteins, and those independent of their homeodomains, are beginning to be described.

We have shown that cell survival following IR was enhanced in four different HOXB7-expressing breast cancer cell lines. Our data indicated enhanced end-joined product formation and enhanced DSB repair (Figs. 2, 5, and 6). When chromosomal damage and cell survival following IR was measured, we found that somewhat less residual damage was apparent in cells expressing HOXB7, an effect that was reversed by *HOXB7* silencing (Fig. 6*A*–*D*). These results indicate that cells expressing HOXB7 have enhanced survival and DNA repair rates compared with nonexpressing controls. The idea that a protein enhancing DNA repair can be an oncogene is somewhat counterintuitive. However, the NHEJ pathway for DNA DSB repair is error-prone compared with that of HR (25). Perhaps HOXB7-expressing cells, which have better survival post-IR exposure and have enhanced NHEJ activity, may harbor more potentially deleterious mutations, leading to a decrease in genomic stability. Enhanced resistance to IR could allow them to accumulate further mutations that initiate tumorigenesis. It would thus be important to determine the genomic integrity and chromosomal stability of these cells.

Interactions similar to the ones reported in this study with Ku were also shown for Werner's syndrome protein (26). In addition, Werner's syndrome protein binds to many other proteins involved in DNA replication and repair, including Rad 52 (27), which we have also found to be associated with HOXB7 immunocomplexes.[6] It is plausible that many other DNA repair–associated proteins form complexes with Ku and PARP, and that this type of complex formation may represent a hallmark of a subset of proteins involved in the same pathway regulating genomic stability. The evidence shown here, indicating roles for HOXB7 in enhanced cell survival and DNA repair rates after irradiation, suggests that HOXB7 joins other important proteins in its involvement in DNA repair and maintenance of genomic stability. Taken together, it seems that HOXB7 may play a novel role in DNA repair by forming complexes with the Ku proteins.

Acknowledgments

Received 11/21/2006; accepted 12/22/2006.

Grant support: DAMD-17-02-1-0426 postdoctoral fellowship grant (E. Rubin and H. Chen), NIH Specialized Programs of Research Excellence grant P50CA88843 and Department of Defense grant COE W81XWH-04-1-0595 (S. Sukumar), and NIH grants (NS34746 and CA10445) and a Department of Defense grant (T.K. Pandita).

The costs of publication of this article were defrayed in part by the payment of page charges. This article must therefore be hereby marked *advertisement* in accordance with 18 U.S.C. Section 1734 solely to indicate this fact.

We thank Kathrin Muegge for generously sharing reagents, Mary Jo Fackler for helpful discussions, and Bert Vogelstein and Alan Rein for critical review of the manuscript.

[6] Our unpublished observations.

References

1. Garcia-Fernandez J. The genesis and evolution of homeobox gene clusters. Nat Rev Genet 2005;6:881–92.
2. Chen H, Sukumar S. Role of homeobox genes in normal mammary gland development and breast tumorigenesis. J Mammary Gland Biol Neoplasia 2003;8:159–75.
3. Topisirovic I, Culjkovic B, Cohen N, Perez JM, Skrabanek L, Borden KL. The proline-rich homeodomain protein, PRH, is a tissue-specific inhibitor of eIF4E-dependent cyclin D1 mRNA transport and growth. EMBO J 2003;22:689–703.
4. Richardson C, Horikoshi N, Pandita TK. The role of the DNA double-strand break response network in meiosis. DNA Repair (Amst) 2004;3:1149–64.
5. Scott SP, Pandita TK. The cellular control of DNA double-strand breaks. J Cell Biochem 2006;99:1463–75.
6. Karran P. DNA double strand break repair in mammalian cells. Curr Opin Genet Dev 2000;10:144–50.
7. Schild-Poulter C, Pope L, Giffin W, et al. The binding of Ku antigen to homeodomain proteins promotes their phosphorylation by DNA-dependent protein kinase. J Biol Chem 2001;276:16848–56.
8. Hochegger H, Dejsuphong D, Fukushima T, et al. Parp-1 protects homologous recombination from interference by Ku and Ligase IV in vertebrate cells. EMBO J 2006;25:1305–14.
9. Schreiber V, Dantzer F, Ame JC, de Murcia G. Poly(ADP-ribose): novel functions for an old molecule. Nat Rev Mol Cell Biol 2006;7:517–28.
10. Zhang X, Zhu T, Chen Y, Mertani HC, Lee KO, Lobie PE. Human growth hormone-regulated HOXA1 is a human mammary epithelial oncogene. J Biol Chem 2003;278:7580–90.
11. Yaron Y, McAdara JK, Lynch M, Hughes E, Gasson JC. Identification of novel functional regions important for the activity of HOXB7 in mammalian cells. J Immunol 2001;166:5058–67.
12. Rubin E, Mittnacht S, Villa-Moruzzi E, Ludlow JW. Site-specific and temporally-regulated retinoblastoma protein dephosphorylation by protein phosphatase type 1. Oncogene 2001;20:3776–85.
13. Shekhar MP, Werdell J, Tait L. Interaction with endothelial cells is a prerequisite for branching ductal-alveolar morphogenesis and hyperplasia of preneoplastic human breast epithelial cells: regulation by estrogen. Cancer Res 2000;60:439–49.
14. Sharma GG, Gupta A, Wang H, et al. hTERT associates with human telomeres and enhances genomic stability and DNA repair. Oncogene 2003;22:131–46.
15. Dhar S, Squire JA, Hande MP, Wellinger RJ, Pandita TK. Inactivation of 14-3-3σ influences telomere behavior and ionizing radiation-induced chromosomal instability. Mol Cell Biol 2000;20:7764–72.
16. Pandita TK, Hittelman WN. Increased initial levels of chromosome damage and heterogeneous chromosome repair in ataxia telangiectasia heterozygote cells. Mutat Res 1994;310:1–13.
17. Story MD, Mendoza EA, Meyn RE, Tofilon PJ. Pulsed-field gel electrophoretic analysis of DNA double-strand breaks in mammalian cells using photostimulable storage phosphor imaging. Int J Radiat Biol 1994;65:523–8.
18. Care A, Felicetti F, Meccia E, et al. HOXB7: a key factor for tumor-associated angiogenic switch. Cancer Res 2001;61:6532–9.
19. Heppner GH, Miller FR, Shekhar PM. Nontransgenic models of breast cancer. Breast Cancer Res 2000;2:331–4.
20. Yavuzer U, Smith GC, Bliss T, Werner D, Jackson SP. DNA end-independent activation of DNA-PK mediated via association with the DNA-binding protein C1D. Genes Dev 1998;12:2188–99.
21. Wayne CM, Sutton K, Wilkinson MF. Expression of the pem homeobox gene in Sertoli cells increases the frequency of adjacent germ cells with deoxyribonucleic acid strand breaks. Endocrinology 2002;143:4875–85.
22. Shiojima I, Komuro I, Mizuno T, et al. Molecular cloning and characterization of human cardiac homeobox gene CSX1. Circ Res 1996;79:920–9.
23. Yang Y, Hwang CK, D'Souza UM, Lee SH, Junn E, Mouradian MM. Three-amino acid extension loop homeodomain proteins Meis2 and TGIF differentially regulate transcription. J Biol Chem 2000;275:20734–41.
24. Hyduk D, Percival-Smith A. Genetic characterization of the homeodomain-independent activity of the Drosophila fushi tarazu gene product. Genetics 1996;142:481–92.
25. Collis SJ, DeWeese TL, Jeggo PA, Parker AR. The life and death of DNA-PK. Oncogene 2005;24:949–61.
26. Li B, Navarro S, Kasahara N, Comai L. Identification and biochemical characterization of a Werner's syndrome protein complex with Ku70/80 and poly(ADP-ribose) polymerase-1. J Biol Chem 2004;279:13659–67.
27. Baynton K, Otterlei M, Bjoras M, von Kobbe C, Bohr VA, Seeberg E. WRN interacts physically and functionally with the recombination mediator protein RAD52. J Biol Chem 2003;278:36476–86.

A Role for the HOXB7 Homeodomain Protein in DNA Repair

Ethel Rubin, Xinyan Wu, Tao Zhu, et al.

Cancer Res 2007;67:1527-1535.